Journal of Nano- and Electronic Physics
Vol. **13** No 2, 02038(6pp) (2021)

Журнал нано- та електронної фізики
Том **13** № 2, 02038(6cc) (2021)

Crystal Structure, Raman Spectra and Electrical Conductivity of $LiNb_{1-x}Ta_xO_3$ Nanopowders Obtained with High-energy Ball Milling

O. Buryy[1,*], L. Vasylechko[1], V. Sydorchuk[2], A. Lakhnik[3], Yu. Suhak[4], D. Wlodarczyk[5], S. Hurskyj[1], U. Yakhnevych[1], Ya. Zhydachevskyy[1,5], D. Sugak[1,6], A. Suchocki[5,7], H. Fritze[4]

[1] *Lviv Polytechnic National University, 12 Bandera St., 79013 Lviv, Ukraine*
[2] *Institute for Sorption and Problems of Endoecology, NASU, 13 Gen. Naumov St., 03164 Kyiv, Ukraine*
[3] *G.V. Kurdyumov Institute of Metal Physics NASU, 36 Acad. Vernadsky Blvd., 03142 Kyiv, Ukraine*
[4] *Institute for Energy Research and Physical Technologies, Clausthal University of Technology, 19B Am Stollen, 38640 Goslar, Germany*
[5] *Institute of Physics PAS, 32/46 Al. Lotnikow, 02668 Warsaw, Poland*
[6] *Scientific Research Company 'Electron-Carat', 202 Stryjska St., 79031 Lviv, Ukraine*
[7] *Institute of Physics, University of Bydgoszcz, 11 Weyssenhoffa St., 85064 Bydgoszcz, Poland*

(Received 15 February 2021; revised manuscript received 15 April 2021; published online 21 April 2021)

The X-ray diffraction, Raman scattering, and the temperature dependences of electrical conductivity are investigated for $LiNb_{1-x}Ta_xO_3$ nanopowders of different composition (x = 0, 0.25, 0.5, 0.75, 1) obtained by mechanochemical synthesis with the use of the planetary ball mill. All samples were thermally treated at 550 °C; in addition, some of them were annealed at 800 °C. The comparison of the obtained structural parameters of $LiNb_{1-x}Ta_xO_3$ samples with the structural data for $LiNbO_3$ and $LiTaO_3$ points to the formation of the $LiNb_{1-x}Ta_xO_3$ solid solution. It is revealed that an increase in Ta content in $LiNb_{1-x}Ta_xO_3$ nanopowders leads to an increase in the a-parameter of the crystal lattice and a simultaneous decrease in the c-parameter that eventually leads to a slight decrease in the unit cell volume. The average size of crystallites varies from 31 nm for the nanopowders annealed only at 550 °C to 206 nm for the ones additionally annealed at 800 °C. It is shown that although the Raman spectra of the investigated nanopowders are similar, some peculiarities are also observed. They arise from the different compositions of nanopowders, as well as from the presence of $LiNb(Ta)_3O_8$, Nb_2O_5 and/or Ta_2O_5 parasitic phases. For the first time, an intense band was revealed in the Raman spectra of samples with $x \neq 0$. This band is observed in the region of 1008…1009 cm^{-1} and, probably, cannot be connected with the presence of parasitic phases. The temperature dependences of pressured $LiNb_{1-x}Ta_xO_3$ nanopowders conductivity are investigated at temperatures of 400…940 °C. The determined activation energies of the electrical conductivity (1.328 eV for x = 0.5, 1.232 eV for x = 0.75, and 1.166 eV for x = 1) are close to the known values for pure $LiNbO_3$ and $LiTaO_3$ in the temperature range of ionic conduction.

Keywords: Nanoparticles, Nanopowders, Lithium niobate-tantalate, X-ray diffraction, Micro-Raman spectroscopy, Temperature dependence of conductivity.

DOI: 10.21272/jnep.13(2).02038 PACS numbers: 61.05.C −, 78.30. − j, 72.20. − i

1. INTRODUCTION

Lithium niobate ($LiNbO_3$, LN) and tantalate ($LiTaO_3$, LT) are among the most frequently used materials of functional electronics. Recently $LiNb_{1-x}Ta_xO_3$ (LN-LT) solid solutions have been studied (see, e.g. [1, 2]), since they offer the prospects for combining the advantages of both materials. Particularly, one can expect that LN-LT will reveal high piezoelectric coefficients (close to those of LN) and temperature stability of properties that is typical for LT. However, the growth of LN-LT single crystals is challenging because of the deviation from stoichiometry that is inherent to LN and LT crystals, non-uniform distribution of cations caused by fluctuations of temperature fields in the area of crystal growth, differences in chemical composition in different parts of the crystal boule, etc. Meanwhile, the nanoparticles of LN-LT can be attractive for practical applications. To date, a large number of works are dedicated to different methods of obtaining LN and LT nanoparticles. The nanoparticles are synthesized at sufficiently low temperatures (300…500 K) that allows to obtain structures with stoichiometric composition, as well as with variation of the concentration ratio [Li]/[Nb] or [Li]/[Ta]. The promising method of LN nanopowder synthesis is high-energy ball milling of lithium carbonate and niobium pentoxide [3]. However, to the best of our knowledge, the nanopowders of LN-LT solid solutions (except for nominally 'pure' LN and LT) have not been investigated to date. Also, we do not know any papers dedicated to mechanochemical synthesis of LT nanopowder.

In this paper, the crystal structure, vibrational spectra and electrophysical properties of LN-LT nanopowders obtained by high-energy ball milling of Li_2CO_3, Nb_2O_5 and Ta_2O_5 as initial reagents are studied. Obtained concentration dependences of the unit cell parameters, Raman spectra and electrical conductivity of $LiNb_{1-x}Ta_xO_3$ series allow to optimize the technological conditions of mechanochemical synthesis of LN-LT solid solution nanoparticles.

2. EXPERIMENTAL DETAILS

Mixed lithium niobate-tantalate nanopowders with nominal compositions $LiNb_{1-x}Ta_xO_3$ (x = 0, 0.25, 0.5, 0.75

* oleh.a.buryi@lpnu.ua

and 1) were obtained by high-energy ball milling of Li_2CO_3, Nb_2O_5 and Ta_2O_5 powder mixtures taken in molar ratios corresponding to stoichiometric compositions.

The synthesis was performed with the planetary ball mill Pulverisette-7. The rotation speed was equal to 600 rpm, and the duration of milling was about 10...15 h. 134 balls of zirconium dioxide with a diameter of 5 mm and a total weight of 91.5 g were used as working bodies. Ball/sample mass ratio was about 10. Milling was performed in 15-min cycles, subsequently, a reverse was carried out after each cycle. Based on the results of previous investigations (see, e.g. [3], where $LiNbO_3$ nanoparticles were synthesized by mechanochemical technique), one can assume that the surfaces of particles were activated, but the synthesis exactly of LN-LT compound was not fully completed after milling. To obtain LN-LT nanoparticles, further annealing of powders was performed. The samples were annealed in air at 550 °C for 5 h and, thereafter, some of them were additionally annealed at 800 °C for 3 h.

Phase compositions of obtained nanoparticles were investigated by X-ray phase analysis using the modernized DRON-3M diffractometer. The crystal structure parameters (unit cell dimensions, positional and displacement parameters of atoms) of both series of materials were derived by full-profile Rietveld refinement using the WinCSD program package for structural analysis [4].

The micro-Raman spectra of LN-LT nanopowders were registered by confocal Raman microscope-spectrometer MonoVista CRS+. The laser beam ($\lambda = 532$ nm) was focused in a 1 μm spot on the surface of pressured nanopowder.

The temperature dependences of electrical conductivity in the range from 400 to 940 °C were obtained by measuring the impedance in the frequency range from 1 Hz to 1 MHz using an impedance gain-phase analyzer. The measurements were carried out on disks (6 mm in diameter and 1.2 mm in thickness) pressured from nanopowders with $x = 0.5$, 0.75 and 1 (the integrity of the other tablets was violated during the experiments). The pressure was about 490 MPa. Subsequently, the obtained discs were annealed in air at 800 °C for 1 h. It should be noted that the reliable results for temperatures lower than 400 °C were not obtained because of too high resistivity of the samples.

3. PHASE COMPOSITION, CRYSTAL STRUCTURE AND MICROSTRUCTURAL PARAMETERS OF $LiNb_{1-x}Ta_xO_3$

X-ray diffraction (XRD) study of all $LiNb_{1-x}Ta_xO_3$ samples synthesized at 550 °C revealed a rhombohedral $LiNbO_3$-type structure as the main phase. However, only the sample with $x = 0$ that corresponds to 'pure' $LiNbO_3$ shows a single-phase composition. In all other $LiNb_{1-x}Ta_xO_3$ samples with x from 0.25 to 1, a certain amount of parasitic phases $Li(Nb, Ta)_3O_8$, Ta_2O_5 and Nb_2O_5 were detected (Table 1). Observable broadening of the Bragg's peaks of the nanocrystalline character of the powders was revealed. Additional heat treatment of the materials at 800 °C led to a narrowing of the diffraction peaks and a considerable change in the phase composition of the $LiNb_{1-x}Ta_xO_3$ samples with x from 0.5 to 1, in which an increase in monoclinic $LiNb_3O_8$ or $Li(Nb, Ta)_3O_8$ phases and the disappearance of individual Ta_2O_5 and Nb_2O_5 oxides were detected (see, e.g. Fig. 1). No significant changes in the phase composition of the samples with $x = 0$ and 0.25 were observed after annealing of the milled samples.

As an example, Fig. 2 demonstrates graphical results of the Rietveld refinement of $LiNb_{0.75}Ta_{0.25}O_3$ material heat-treated at 800 °C.

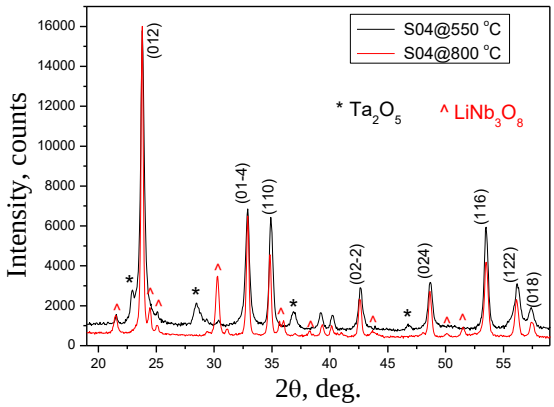

Fig. 1 – Fragment of XRD patterns of S04 sample of nominal composition $LiNb_{0.25}Ta_{0.75}O_3$ heat-treated at 550 and 800 °C. For the main rhombohedral LN-LT phase, the Miller's indices are given

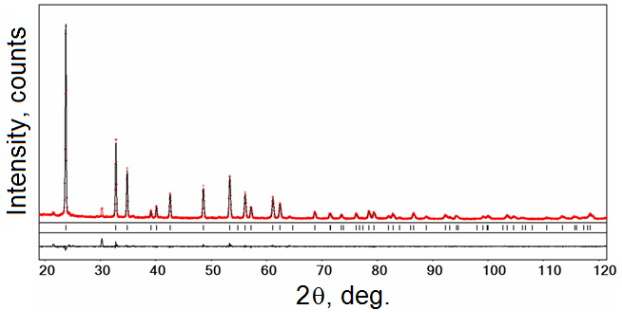

Fig. 2 – Graphical results of the Rietveld refinement of the $LiNb_{0.75}Ta_{0.25}O_3$ material heat-treated at 800 °C. Experimental XRD pattern (dots) is shown in comparison with the calculated pattern. The difference between measured and calculated profiles is shown as a curve below the diagram. Short vertical bars indicate the positions of the diffraction maxima in space group $R3c$

Analysis of the obtained structural parameters revealed that an increase in Ta content in both series of $LiNb_{1-x}Ta_xO_3$ specimens leads to an increase in the a-parameter and a simultaneous decrease in the c-parameter (Fig. 3a). As a result, a significant decrease in the c/a ratio and a minor decrease in the unit cell volume in both $LiNb_{1-x}Ta_xO_3$ series are observed. Interestingly, similar to the compositional effect on the unit cell dimensions of $LiNb_{1-x}Ta_xO_3$ materials, there was an increase in the heat treatment temperature from 550 to 800 °C, which led to an increase in the a-parameter and a simultaneous reduction in the c-parameter (Fig. 3).

Table 1 – Lattice parameters (a, c), average grain size D_{ave} and microstrain values (<ε>) of two $LiNb_{1-x}Ta_xO_3$ series heat-treated at 550 and 800 °C

Sample	x	T, °C	Parasitic phases	a, Å	c, Å	D_{ave}, nm	<ε>, %
S01	0	550	–	5.1483(3)	13.8484(9)	41	0.088
		800	–	5.1517(2)	13.8335(7)	206	0.108
S02	0.25	550	$Li(Nb, Ta)_3O_8$	5.1477(3)	13.822(1)	50	0.143
		800	$Li(Nb, Ta)_3O_8$	5.1521(3)	13.8148(8)	171	0.105
S03	0.5	550	$Ta_2O_5 + LiNb_3O_8$	5.1534(4)	13.808(1)	63	0.107
		800	$Li(Nb, Ta)_3O_8$	5.153(1)	13.778(3)	97	0.128
S04	0.75	550	Ta_2O_5	5.149(2)	13.788(5)	31	0.093
		800	$Li(Nb, Ta)_3O_8$	5.1558(7)	13.753(2)	92	0.139
S05	1	550	Ta_2O_5	5.1529(6)	13.767(2)	66	0.114
		800	$Li(Nb, Ta)_3O_8$	5.1593(4)	13.745(2)	80	0.135

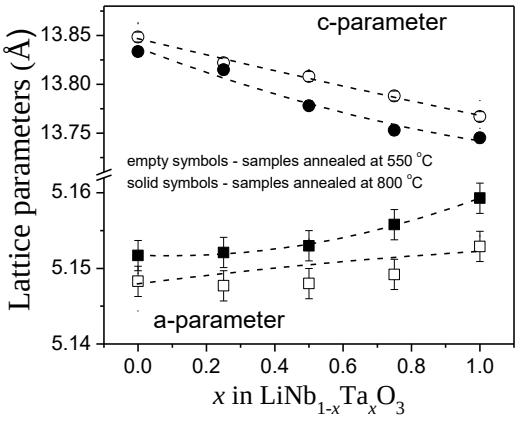

a

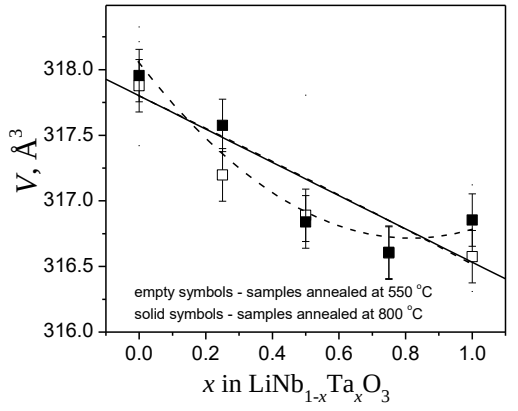

b

Fig. 3 – Concentration dependences of the lattice parameters (a, c) and the unit cell volume in $LiNb_{1-x}Ta_xO_3$@550C and $LiNb_{1-x}Ta_xO_3$@800C series. The dashed lines are a guide for eyes

The comparison of the obtained structural parameters of LN-LT samples with the corresponding structural data for nominally pure LN and LT [5, 6] points to the formation of the continuous $LiNb_{1-x}Ta_xO_3$ solid solution.

4. INVESTIGATION OF THE RAMAN SPECTRA OF $LiNb_{1-x}Ta_xO_3$ NANOPOWDERS

The micro-Raman spectra of LN-LT nanopowders with different Nb and Ta content, annealed at 550 °C are shown in Fig. 4. As it is seen from this figure, the Raman spectra of LN-LT with different x are generally similar, however some peculiarities are observed. Particularly, in the spectrum of pure LN, 15 Raman bands can be distinguished, 11 of which can be attributed to A_1 and E vibrational modes. The A_1 modes are polarized along the Z-axis, while the doubly degenerate E modes correspond to ionic motions along the X or Y-axis [7 8]. In the spectrum of LN-LT ($x = 0.25$), 25 Raman bands can be distinguished, for $x = 0.5$ the number of bands is equal to 20, for $x = 0.75$ – to 15 and for pure LT – to 17. The differences in the number of distinguished bands could probably be caused by the overlapping of some bands with those with higher intensity. The observed differences could be explained by the different composition of nanopowders, as well as by probable non-optimality of technological regimes of nanopowder synthesis. Particularly, the following main specific features of the Raman spectra of LN-LT nanopowders were revealed.

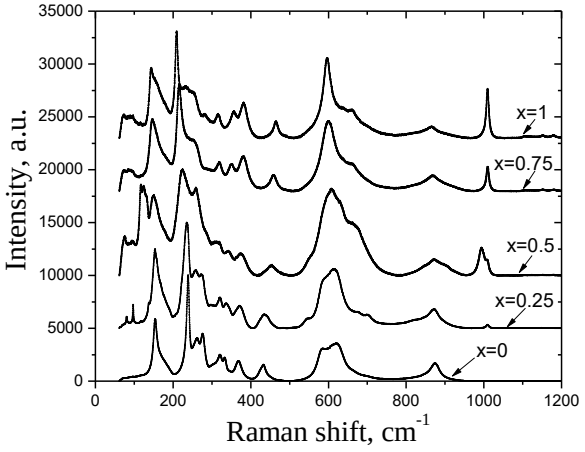

Fig. 4 – Raman spectra of $LiNb_{1-x}Ta_xO_3$ nanopowders

(1) A few low-frequency bands near 73…75 and 90…97 cm^{-1} are observed for the nanopowders with $x \neq 0$. These bands cannot be associated with known Raman bands of LT [7-9]. In accordance with the results of [16], these bands could be induced by the presence of $Li(Nb, Ta)_3O_8$ phase identified by X-ray diffraction technique (see Table 1).

(2) A more intense band near 117…125 cm^{-1} is observed only for the LN-LT sample with $x = 0.5$. The presence of this band could be attributed to the contribution of $Li(Nb, Ta)_3O_8$ and Ta_2O_5 additional phases in this sample. Note, that the authors of [10] observed the

close bands at 116 and 136 cm^{-1} and attributed them to $LiNb_3O_8$. The bands near 100 cm^{-1} were attributed to Ta_2O_5 by the authors of [11]. As follows from the XRD data (see Table 1), the simultaneous presence of the $Li(Nb, Ta)_3O_8$ and Ta_2O_5 phases occurs only in the sample with $x = 0.5$, so the overlapping of the corresponding bands can result in a peculiar form of its spectrum. Furthermore, the sample with $x = 0.5$, i.e., with a composition intermediate between pure LN and pure LT, ought to essentially reveal the bands of both crystals, so it is no wonder that the spectrum of this sample has the most complex character.

Further, the sample with $x = 0.5$ reveals a significant increase in the band intensities near 260 and 630…670 cm^{-1} that visually looks like an expansion of intense neighboring peaks. This result is in good agreement with [12], where two intense neighboring bands in the region of 600 cm^{-1} were also observed for the LN-LT sample with $x = 0.553$.

Finally, it should be noted that the bands near 600 cm^{-1} are considerably broad for all investigated samples in comparison with the other observed bands. This is consistent with the results of [13], where it is concluded that the band at 600 cm^{-1} is broader for non-poled LN samples (particularly, nanopowders) than for polarized.

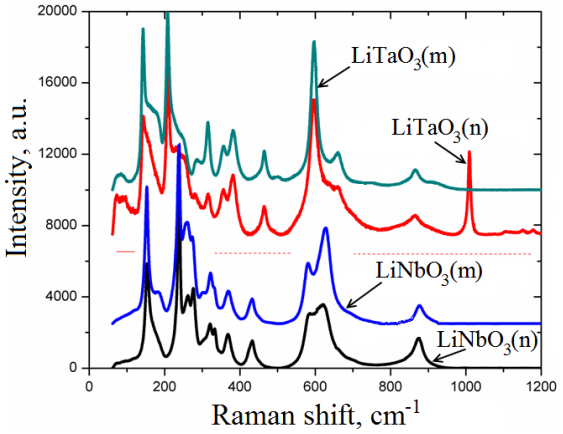

Fig. 5 – Raman spectra of nanopowders (n) of $LiNbO_3$ and $LiTaO_3$ synthesized by mechanochemical treatment and the ones of micropowders (m) of $LiNbO_3$ and $LiTaO_3$ obtained by crushing

(3) The Raman spectra of LN and LT nano- and micropowders are shown in Fig. 5 for comparison purposes. The latter were obtained by crushing LN and LT single crystals grown at the SRC "Electron-Carat". As seen from Fig. 5, the band observed in the range 1008…1009 cm^{-1} for LT nanopowder is not pronounced for LT micropowder, as well as for LN compounds. A similar band can be observed in Fig. 4 for nanopowders with $x \neq 0$. As it is seen from Fig. 4, the intensity of this band increases with increasing x. Moreover, for $x = 0.5$ this band splits into two with the frequencies of 994 and 1008 cm^{-1}. As shown in [11], this band is absent in Ta_2O_5 Raman spectrum. Since the data about Raman scattering in $LiNb_3O_8$ are not available in this spectral range, we cannot exclude that this band is associated with $LiNb_3O_8$ (or $LiTa_3O_8$) phase. However, as it is seen from Table 1, $LiTa_3O_8$ phase is absent in pure LT sample annealed at 550 °C, as well as in the sample with $x = 0.75$ (within the limits of accuracy). Thus, we have to conclude that the nature of this band cannot be clearly determined from current experiments and requires additional studies.

(4) Contrary to the results of [14], we did not observe any remarkable effect of grain size reduction, i.e., a decrease in the intensities of all Raman bands caused by a decrease in the grain size (Fig. 5).

(5) An increase in the spectral range up to 4000 cm^{-1} allows to reveal weak vibrations at 1600 and 3400 cm^{-1} (looking like low-intensity broad bands) that can be caused by traces of OH^- groups, which are always present in LN and LT, as well as traces of HCO_3^- groups (about 1750 and 2900 cm^{-1}) present in the synthesized compounds, probably due to the use of lithium carbonate as a component of the initial mixture.

5. ELECTRICAL PROPERTIES OF $LiNb_{1-x}Ta_xO_3$ NANOPOWDERS

The temperature dependences of the conductivity σ of pressured $LiNb_{1-x}Ta_xO_3$ nanopowders in the temperature range up to 940 °C are presented in Fig. 6 and are qualitatively the same as those given for LN-LT micropowders obtained by solid-state reaction in [15]. However, the sequence of dependences along the ordinate axis in Fig. 6 coincides with that indicated in [15] only in the temperature range up to temperatures of about 730 °C ($10^4/T \approx 10$ K^{-1}), whereas at higher temperatures the conductivity of the sample with $x = 0.5$ exceeds the one of the sample with $x = 1$ (in [15], the relationship between the samples conductivities is $\sigma_{x=0.75} < \sigma_{x=0.5} < \sigma_{x=1}$ over the entire investigated temperature range up to 850 °C). Probably, this difference is caused by the dependence of LN-LT properties on sizes of the powder grains which are different in our work and in [15].

The temperature dependences of conductivities have an activation character. No remarkable peculiarities are observed for the samples with $x = 0.5$ and 0.75, whereas for pure LT ($x = 1$) a slight kink is observed at temperatures of about 680…700 °C. It is possible that this peculiarity is caused by the transition from the ferroelectric to the paraelectric phase, the temperature of which varies from 577 to 697 °C and depends on the stoichiometric composition of the crystal [16].

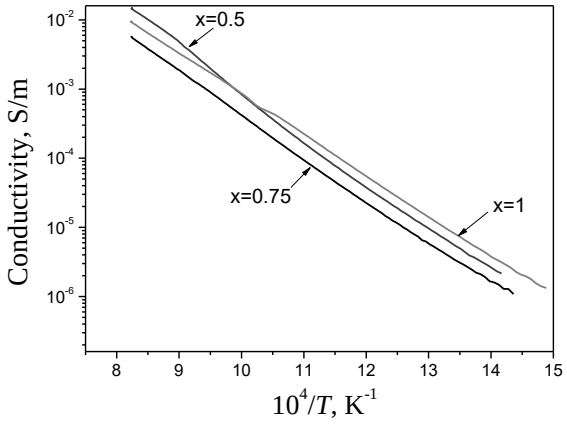

Fig. 6 – Temperature dependences of the conductivity of pressured $LiNb_{1-x}Ta_xO_3$ nanopowders with different compositions

The activation energy of electrical conductivity $\Delta E = -kT\ln(\sigma/\sigma_0)$ is equal to $\Delta E = 1.328 \pm 0.005$ eV ($x = 0.5$), $\Delta E = 1.232 \pm 0.003$ eV ($x = 0.75$) and $\Delta E = 1.166 \pm 0.001$ eV ($x = 1$), so it slightly decreases with increasing Ta content. As it is seen from Fig. 6, $\sigma(T)$ dependences in the Arrhenius plot deviate slightly from straight lines (this is particularly visible for $x = 0.5$), however these deviations do not reflect changes in the conductivity mechanism. In particular, the activation energy $\Delta E = 1.230 \pm 0.003$ eV corresponds to the high-temperature part of the $\sigma(T)$ dependence for $x = 0.5$ (at $T > 843$ °C or $10^4/T < 10.39$ K^{-1}, a certain kink of the corresponding curve in Fig. 6 is observed at this value), whereas for the low-temperature ($T < 843$ °C) part of this dependence the activation energy is equal to 1.298 ± 0.007 eV, so both values coincide in the frames of the error.

It should be noted that the authors of [17, 18] obtained different activation energies for LT single crystals in the temperature ranges of 390…450 K and 550…900 K. At that, two types of carriers with activation energies of 0.29 eV and 1.03 eV contribute to the conductivity in the low-temperature range and one type with an activation energy of 1.34 eV – to the conductivity at $T > 550$ K. The corresponding mechanisms of conductivity were attributed to proton conduction, electron hopping and ionic conduction, respectively [17]. Since in our experiments the temperature dependences of the conductivity were measured above 400 °C, it is not surprising that we observed only ionic conduction with activation energies close to those determined in [18]. The close values of activation energies were also obtained in [19] for $LiTaO_3$ and in [20] for stoichiometric $LiNbO_3$.

6. CONCLUSIONS

The samples of $LiNb_{1-x}Ta_xO_3$ ($x = 0$, 0.25, 0.5, 0.75, 1) nanopowder were obtained by mechanochemical synthesis with the use of the planetary ball mill. After milling, the samples were annealed at 550 °C and, thereafter, some of them were additionally annealed at 800 °C.

The phase compositions of the samples were determined by X-ray diffraction technique. The full-profile Rietveld refinement was used for the determination of the crystal structure parameters and microstructure parameters of $LiNb_{1-x}Ta_xO_3$ nanopowders. It is shown that the replacement of niobium by tantalum in the $LiNb_{1-x}Ta_xO_3$ structure asymmetrically affects the parameters of the unit cell: an increase in Ta content leads to an increase in the lattice parameter a, and a simultaneous decrease in the parameter c is accompanied by a slight decrease in the unit cell volume. It is shown that the average size of crystallites varies from 31 nm (treatment only at 550 °C) to 206 nm (additional treatment at 800 °C) for different nanopowder samples.

Raman scattering in nanopowders ($x = 0$, 0.25, 0.5, 0.75, 1) obtained by high-energy ball milling technique was investigated for the first time. As shown, the obtained Raman spectra are generally similar. Some peculiarities (shifts of bands, changes in their intensities, formation of new bands) are caused by different compositions and the presence of $LiNb(Ta)_3O_8$, Nb_2O_5 and/or Ta_2O_5 parasitic phases. An intense band at about 1008…1009 cm^{-1} for nanopowders with $x \neq 0$ was not previously observed in single crystals or ceramics of $LiNbO_3$ and $LiTaO_3$ and, probably, is not caused by the presence of parasitic phases. Thus, the determination of the nature of this band requires further investigations.

The temperature dependences of the conductivities of the investigated $LiNb_{1-x}Ta_xO_3$ samples reveal an activation character. The activation energy slightly decreases with increasing tantalum content from 1.328 ± 0.005 eV for $x = 0.5$ to 1.166 ± 0.001 eV for $x = 1$ (pure LT) and corresponds to the conductivity mechanism of ionic conduction.

ACKNOWLEDGEMENTS

The work was carried out in the framework of the joint German-Ukrainian project "Nanocrystalline piezoelectric compounds $LiNb_{1-x}Ta_xO_3$ for high-temperature applications" (M/48-2020). This research was partially supported by the Ministry of Education and Science of Ukraine through the project DB/KINETYKA (No 0119U002249), as well as through the grant No 2019/33/B/ST8/02142 of the Polish National Science Center.

REFERENCES

1. I.G. Wood, P. Daniels, R.H. Brownand, A.M. Glazer, *J. Phys.: Condens. Matter* **20**, 235237 (2008).
2. A. Bartasyte, A.M. Glazer, F. Wondre, D. Prabhakaran, P.A. Thomas, S. Huband, D.S. Keebleand, S. Margueron, *Mater. Chem. Phys.* **134**, 728 (2012).
3. S. Khalameida, V. Sydorchuk, R. Leboda, J. Skubiszewska-Zięba, V. Zazhigalov, *J. Therm. Anal. Calorim.* **115**, 579 (2014).
4. L. Akselrud, Yu. Grin, *J. Appl. Crystallography* **47**, 803 (2014).
5. M. Ohgaki, K. Tanaka, F. Marumo, *Mineral. J.* **16**, 150 (1992).
6. N. Iyi, K. Kitamura, F. Izumi, J.K. Yamamoto, T. Hayashi, H. Asano, S. Kimura, *J. Sol. State Chem.* **101**, 340 (1992).
7. V.S. Gorelik, S.D. Abdurakhmonov, N.V. Sidorov, M.N. Palatnikov, *Inorg. Mater.* **55**, 524 (2019).
8. A. Ridah, P. Bourson, M.D. Fontana, G. Malovichko, *J. Phys. Cond. Matter* **9**, 9687 (1997).
9. Y. Repelin, E. Husson, F. Bennani, C. Proust, *J. Phys. Chem. Solids* **60**, 819 (1999).
10. A. Bartasyte, V. Plausinaitiene, A. Abrutis, Sandra Stanionyte, S. Margueron, P. Boulet, T. Kobata, Y. Uesu, J. Gleize, *J. Phys.: Condens. Matter* **25**, 205901 (2013).
11. N. Verma, B. Mari, K.C. Singh, J. Jindal, M. Mollar, R. Rana, A.L.J. Pereira, F.J. Manjón, *AIP Conf. Proc.* **1724**, 020082 (2016).
12. M. Rüsing, S. Sanna, S. Neufeld, G. Berth, W.G. Schmidt, A. Zrenner, H. Yu, Y. Wang, H. Zhang, *Phys. Rev. B* **93**, 184305 (2016).
13. A. Golubović, R. Gajić, I. Hinić, M. Šćepanović, *J. Alloy. Compd.* **460**, 74 (2008).
14. P. Heitjans, M. Masoud, A. Feldhoff, M. Wilkening, *Faraday Discuss* **134**, 67 (2007).
15. K.Y. Bak, K.B. Tan, C.C. Khaw, Z. Zainal, P.Y. Tan, M.P. Chon, *Sains Malaysiana* **43**, 1573 (2014).
16. A.M. Pugachev, S. Kojima, H. Anwar, *Phys. Solid State* **48**, 1050 (2006).

17. A.V. Yatsenko, M.N. Palatnikov, O.V. Makarova, N.V. Sidorov, S.V. Yevdokimov, *Ferroelectrics* **477**, 47 (2015).
18. M.N. Palatnikov, A.V. Yatsenko, V.A. Sandler, N.V. Sidorov, D.V. Ivanenko, O.V. Makarova, *Inorg. Mater.* **53**, 576 (2017).
19. A. Huanosta, A.R. West, *J. Appl. Phys.* **61**, 5386 (1987).
20. A. Weidenfelder, J. Shi, P. Fielitz, G. Borchardt, K.D. Becker, H. Fritze, *Solid State Ion.* **225**, 26 (2012).

Кристалічна структура, спектри комбінаційного розсіювання та електрична провідність нанопоршків $LiNb_{1-x}Ta_xO_3$, отриманих за методом високоенергетичного розмелювання на кульовому млині

О. Бурий[1], Л. Василечко[1], В. Сидорчук[2], А. Лахнік[3], Ю. Сугак[4], Д. Влодарчик[5], С. Гурський[1], У. Яхневич[1], Я. Жидачевський[1,5], Д. Сугак[1,6], А. Сухоцький[5,7], Х. Фрітце[4]

[1] *Національний університет «Львівська політехніка», вул. Бандери, 12, 79013 Львів, Україна*
[2] *Інститут сорбції та проблем ендоекології НАНУ, вул. ген. Наумова, 13, 03164 Київ, Україна*
[3] *Інститут металофізики імені Г.В. Курдюмова НАНУ, бульв. акад. Вернадського, 36, 03142 Київ, Україна*
[4] *Інститут енергетичних досліджень та фізичних технологій, Університет технологій Клаусталь, 19B Ам Штолен, 38640 Гослар, Німеччина*
[5] *Інститут фізики ПАН, ал. Лотніков, 32/46, 02668 Варшава, Польща*
[6] *Науково-дослідне підприємство «Електрон-Карат», вул. Стрийська, 202, 79031 Львів, Україна*
[7] *Інститут фізики, Університет Бидгоща, вул. Вейссенхоффа, 11, 85064 Бидгощ, Польща*

Досліджено рентгенівську дифракцію, комбінаційне розсіювання та температурні залежності електричної провідності нанопорошків $LiNb_{1-x}Ta_xO_3$ різного складу (x = 0, 0.25, 0.5, 0.75, 1), отриманих за методом механосинтезу з використанням планетарного кульового млина. Всі зразки відпалювалися за температури 550 °C; крім того, ряд зразків було додатково відпалено при 800 °C. Порівняння отриманих структурних параметрів зразків $LiNb_{1-x}Ta_xO_3$ із структурними даними для $LiNbO_3$ та $LiTaO_3$ вказує на утворення твердого розчину $LiNb_{1-x}Ta_xO_3$. Встановлено, що збільшення вмісту Ta у нанопорошках $LiNb_{1-x}Ta_xO_3$ веде до збільшення параметра a кристалічної решітки за одночасного зменшення параметра c, що в цілому призводить до деякого зменшення об'єму елементарної комірки. Середній розмір кристалітів змінюється від 31 нм для нанопорошків, відпалених лише при 550 °C, до 206 нм для нанопорошків, додатково відпалених при 800 °C. Показано, що хоча спектри комбінаційного розсіювання досліджених нанопорошків є подібними, деякі особливості також мають місце. Вони пов'язані як з різними складами нанопорошків, так і з присутністю паразитних фаз $LiNb(Ta)_3O_8$, Nb_2O_5 та/або Ta_2O_5. Вперше виявлено інтенсивну смугу комбінаційного розсіювання зразків з $x \neq 0$. Ця смуга спостерігається в області 1008…1009 $см^{-1}$ і, імовірно, не є пов'язаною з присутністю паразитних фаз. Температурні залежності провідності пресованих нанопорошків $LiNb_{1-x}Ta_xO_3$ досліджено в температурному інтервалі 400…940 °C. Визначені енергії активації електричної провідності (1.328 еВ для x = 0.5, 1.232 еВ для x = 0.75 та 1.166 еВ для x = 1) є близькими до відомих величин для чистих $LiNbO_3$ та $LiTaO_3$ у температурному діапазоні іонної провідності.

Ключові слова: Наночастинки, Ніобат-танталат літію, Рентгенівська дифракція, Мікро-раманівська спектроскопія, Температурна залежність провідності.